Influence of knots and density distribution on compressive strength of wooden foundation piles

Pagella, G.; Mirra, M.; Ravenshorst, G. J.P.; Van De Kuilen, J. W.G.

DOI
10.1201/9781003348443-277

Publication date
2023

Document Version
Final published version

Published in
Current Perspectives and New Directions in Mechanics, Modelling and Design of Structural Systems - Proceedings of the 8th International Conference on Structural Engineering, Mechanics and Computation, 2022

Influence of knots and density distribution on compressive strength of wooden foundation piles

G. Pagella, M. Mirra & G.J.P. Ravenshorst
Delft University of Technology, Delft, The Netherlands

J.W.G. van de Kuilen
Technical University of Munich, Munich, Germany & Delft University of Technology, Delft, The Netherlands

ABSTRACT: This work investigated the influence of knots on the compression strength of wooden foundation piles. The study involved 110 pile segments sawn from 18 spruce and 9 pine piles with a mean diameter of approximately 200 mm, and moisture contents above fiber saturation. The mechanical properties were determined performing both full-scale compression tests on pile segments, and small-scale experiments on discs sawn from selected segments, considering samples with and without knots. A knot ratio (KR) was defined analysing the knots layout of each wooden pile, and evaluating how the compressive strength was influenced by size, number and layout of knots. As final step, a prediction model was implemented based on the dry density and KR of wooden piles, to estimate the influence of knots on their compressive strength.

1 INTRODUCTION

For engineering purposes, structural sawn timber is assigned to a strength class. To achieve this, timber boards are visually or machine graded. Grading parameters can be knots or modulus of elasticity and/or density. By defining limits for the magnitude in which these grading features may occur, for instance maximum knot size in the case of visual grading, timber boards can be assigned to different strength classes (Ravenshorst 2015). However, for timber piles, one strength class based on visual grading is defined in Dutch standard NEN 5491 (2010). The grade boundary relates to the declared characteristic value in compression, determined on the basis of tests performed on wooden piles with knots (van de Kuilen 1994). This study mainly consisted in tests on pile heads, without providing values in compression for the full pile. Therefore, this paper investigates the influence of knots on the compressive strength along wooden piles, as part of the research regarding the current state of existing foundation piles in Amsterdam (van de Kuilen et al. 2021), (Pagella et al. 2022), for a better understanding of the reference quality of the material. However, the high variability and heterogeneity of the material, due to specific natural growth characteristics of trees, is the reason for complexity in the determination of the mechanical properties of wooden piles (Vieira Rocha et al. 2018), (Hossein et al. 2011). Growth characteristics such as grain deviations, tapered shape, geometry imperfections and knots, result to have large influence on mechanical properties. In the case of a wooden pile, subjected to axial load during its service life, the presence of knots can be governing for the capacity of the pile. This is because the low stiffness of the cross section with knots in the axial direction of a pile, due to fiber deviation around a knot, implies that only a very small amount of the load is taken up by the knots. In addition, it was assumed that the zone around the knot, where the fibers in longitudinal direction deviate, has a slightly higher stiffness than the knot itself, but still very low. Therefore, the influence of knots as a strength-reducing factor on the load bearing capacity of timber piles has been studied over the length of the pile. Based on experimental tests, a model to predict the compressive strength along the pile will be presented.

2 MATERIALS AND METHODS

2.1 *Materials*

In this research, the following full-scale specimens have been investigated:

- 18 spruce (*picea abies*) piles from the Netherlands;
- 9 pine (*pinus sylvestris*) piles from Germany.

All piles were felled in 2019, had an average length of 14 meters, average head diameter of 255 mm and average tip diameter of 145 mm. The piles were driven into the ground in a test field in Amsterdam with the main objective to determine geotechnical parameters. In spring 2021, the wooden piles were extracted from the location and tested over the whole length with frequency response measurements,

to determine the dynamic modulus of elasticity (MOE_{dyn}). The 27 piles were cut in three parts and transported to the TU Delft Stevin 2 laboratory. At the arrival, all the piles were cut into 110 segments with a length of approximately six times the average diameter. For most piles, three segments (sawn from the head, middle and tip part) were tested according to the procedure described in section 2.2. For six piles, eight segments over the length of the piles were tested to gain insight into a more precise distribution of knots and strength along the pile. Finally, for three segments that were tested, two discs of 100 mm length were sawn:

- one disc without knots;
- one disc with a branch whorl.

A branch whorl is defined in ISO 24294 (2021) as the zone of the stem where several branches or knots occur at approximately the same cross section.

2.2 *Methods*

2.2.1 *Compression tests on segments*

The length of the pile segments was calculated depending on the diameter of the average cross section of each pile. Three length categories were established: 900 mm, 1350 mm and 1800 mm, according to EN 408 (2010) and EN 14251 (2003), which prescribe an axial length of six times the smaller diameter of the cross section for a pile. Before the compression test, the piles were constantly kept under water to achieve a wet saturated condition with an average moisture content value of 70% with variations of ± 20%. This was done to recreate the same in-soil conditions where the piles were fully under the water table, in order to retrieve comparable mechanical and physical properties during the compression test. The moisture content was estimated with the oven-dry method, according to EN 13183 (2002), for two 30 mm thick discs taken from both sides of each selected segment.

Before running the mechanical tests, the pile segments were taken out of the water and weighted, and the density of each pile was measured by determining volume and wet mass (EN 384 2016) from which the moisture content was determined. Mechanical testing was performed to determine compression strength ($f_{c,0,meas,wet}$). The index *meas* is used to distinguish from modelled values. All compression strength values, measured and modeled, refer to the full cross-sectional area. A displacement controlled set-up was used (Fig. 1), where the specimens were subjected to an axial load in direction parallel to the fibers (EN 408 2010), (EN 14251 2003). The displacement between the two steel plates was monitored with four linear potentiometers placed on the four edges of the top plate and connected to the bottom plate. The deformation of the specimens was measured with six linear potentiometers screwed on the surface. Four of them were placed on each side of the pile, 90° from each other, with a variable length equal to two-thirds of the length of the specimen. The other two sensors were placed over a knot and on a clear-wood part, in order to evaluate the deformation with and without the influence of a knot. At the end of the test, $f_{c,0,meas,wet}$ was calculated from the ratio between the maximum force reached in compression by the specimen and the average cross-sectional area of the pile.

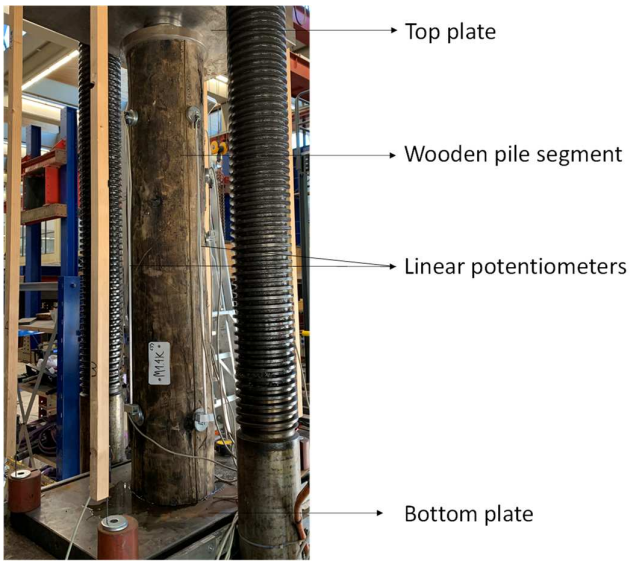

Figure 1. Set-up for mechanical testing of pile segments.

2.2.2 *Determination of the knot area*

According to EN 1309-3 (2018) and NEN 5461 (2011), the method for the classification of knots depends on the type of knot (round, oval, arris, etc.) and it is established for timber beams. The size of a knot is indicated as the width of the knot or knot cluster, measured perpendicularly to the longitudinal axis of the piece. However, this method does not take into account the influence of knots on the fiber orientation. The area around the knot with a fiber angle deviating from the longitudinal axis will have a lower stiffness than the fibers running parallel to the longitudinal axis. Thus, the knots layout of the specimens was studied calculating both the diameter of the knot itself (Φ_1) and the diameter around the knot where fiber deviations were visible ($\Phi_1 + \alpha\,\Phi_1$) (Fig. 2). In this way, also the influence on the stress distribution of areas where fibers are not parallel to the axial load could be considered. The surface of each wooden pile was mapped calculating Φ_1 and $\alpha\Phi_1$ of each knot on the longitudinal axis. Subsequently, an equivalent knot diameter Φ_2 was defined as the diameter to which no strength is accounted for the prediction models described in section 4. The equivalent diameter Φ_2 is calculated with equation 1.

$$\Phi_2 = \Phi_1 + \alpha\,\beta\,\Phi_1 \quad (1)$$

The coefficient α is a pure geometrical factor, taking into account the size of the fiber deviation around a knot, which is visually measured.

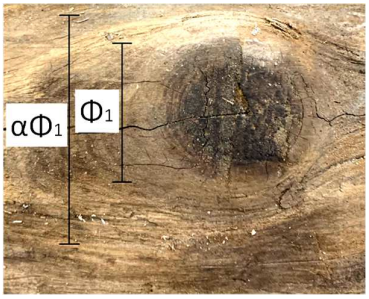

Figure 2. Calculation of the diameter of a wood knot: Φ_1 is the diameter of the knot itself; $\alpha\Phi_1$ is the diameter referred to the grain deviation caused by the knot.

The factor β describes how much of $\alpha\Phi_1$ should be taken into account to obtain a value for Φ_2 as an equivalent size to which no strength is assigned. The knots distribution along the length of each tapered wooden pile was studied in correlation with the circumference of the specimens. In order to study how the knots layout may influence $f_{c,0,meas,wet}$, a knot ratio (KR) was defined as the sum of the diameters $\Phi_{2,i}$ of each knot in a branch whorl within a section of a pile (usually a branch whorl is visible over a length of 100 mm) and the circumference *O* of that pile (Eq. 2). In addition, KR was calculated considering Φ_1, to investigate the difference in correlation with $f_{c,0,meas,wet}$.

$$KR = \frac{\sum_{i=1}^{n} \Phi_{2,i}}{O} \quad (2)$$

In more than 70% of pile segments, the failure occurred in the section with the highest number and/or bigger size of knots. Based on this, the maximum KR measured in a pile segment was considered for this study. KR was calculated with reference to a specific section of the pile where knots could affect the strength and lead to a premature failure. The influence of KR on $f_{c,0,meas,wet}$ was investigated: the compressive strength of pile segments without visible knots on the surface was compared with all other pile segments with knots. The reference value for $f_{c,0,meas,wet}$ of samples without knots, was determined performing large-scale testing on five pile segments.

2.2.3 *Compression tests on discs*

The global analysis was validated by testing also three 100-mm-thick wooden discs sawn from a section without knots, i.e. a clear wood section of the same pile segments, characterized by a compressive strength $f_{c,0,CW,meas,wet}$. Moreover, other three discs where sawn in correspondence to a section with maximum KR of the same pile segments, to further analyze the influence of knots on compressive strength $f_{c,0,KR,meas,wet}$ with local tests (Fig. 3), besides the large-scale ones.

All discs were subjected to compression load until failure measuring the deformation with four linear potentiometers attached on the pile surface (Fig 4). From these tests, reference values of $f_{c,0,CW,meas,wet}$ for pile sections without knots and $f_{c,0,KR,meas,wet}$ for pile sections with knots were determined.

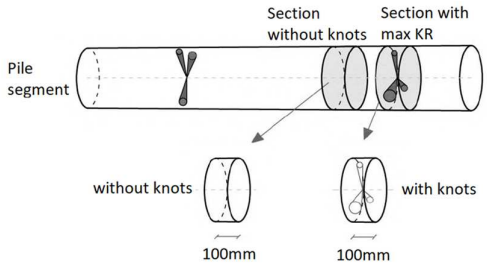

Figure 3. Discs with and without knots sawn from a pile segment in correspondence to a clear wood section (without knots) and a section with maximum KR.


Figure 4. Compression test of a disc sawn from a pile segment.

Furthermore, additional six full-length piles were divided in eight sub-parts and tested in compression, to collect data regarding the mechanical properties of each sub-part and their correlation with knots layout.

3 RESULTS

3.1 *Relationship between Φ_1 and $\alpha\Phi_1$*

The aforementioned coefficient α, determined by visual measurements, is shown in Table 1. From the classes of knots, it is possible to observe that larger knots contributed less to fiber deviation. Therefore, in the tip of a pile, where generally knots were found more frequently but the circumference was smaller, a knot had a more severe influence on the fiber deviation and thus on the compressive strength. However, it should be considered that a larger amount of juvenile wood is also present in the tip.

Table 1. Coefficient α in relation to Φ_1, determined according to the conducted visual measurements.

Class of knots	α	Diameter Φ_1
	-	mm
A	1.39	$\Phi_1 < 15$
B	1.19	$15 \leq \Phi_1 \leq 20$
C	0.97	$21 \leq \Phi_1 \leq 25$
D	0.93	$26 \leq \Phi_1 \leq 30$
E	0.86	$\Phi_1 > 30$

3.2 *Compression strength and KR values of segments*

The average mechanical properties of 110 pile segments were obtained: Table 2 shows the distribution of dry density (ρ_{dry}), moisture content (m.c.), KR and $f_{c,0,meas,wet}$ along the pile, by subdividing the specimens in head, middle-part and tip. The results showed an average decrease of $f_{c,0,meas,wet}$ from the head to the

tip. In particular, for heads and middle-parts, the average $f_{c,0,meas,wet}$ was comparable, while for tips a 20% reduction was measured. This can be attributed to an observed larger number of knots in tips and thus higher KRs. Another aspect is related to a larger presence of juvenile wood in the tip of a pile, which could influence the compressive strength, especially in the very tip.

Table 2. Average mechanical properties of the tested 110 pile segments. In brackets the standard deviation is reported.

Segments	Avg. ρ_{dry} kg/m^3	Avg. m.c %	Avg. KR Φ_2 -	Avg. $f_{c,0,meas,wet}$ MPa
Head	400 (43)	87 (14)	0.14 (0.07)	16.7 (3.4)
Middle	395 (24)	78 (10)	0.21 (0.05)	16.3 (1.7)
Tip	390 (25)	80 (10)	0.28 (0.08)	14.9 (1.9)
All	395 (33)	82 (12)	0.22 (0.09)	16.0 (2.5)

3.3 *Compression strength and KR values of discs*

The results of six wooden discs with and without knots are presented in relation to their pertaining pile segment in Table 3. For discs without knots, an average $f_{c,0,CW,meas,wet}$ of 21.6 MPa was obtained, in line with the average value of 21.5 MPa determined for the five pile segments without knots. Besides, it is possible to observe how $f_{c,0,KR,meas,wet}$ of discs with knots (at different KRs) is comparable with $f_{c,0,KR,meas,wet}$ obtained testing in compression the three pile segments (see again Tab. 3).

Table 3. Compressive strength of pile segments and relative discs with and without knots.

Sample	Code -	KR Φ_2 -	$f_{c,0,CW,meas,wet}$ MPa	$f_{c,0,KR,meas,wet}$ MPa
Segments	1	0.27	-	15.5
	2	0.31	-	15.5
	3	0.27	-	13.3
Discs	1a	0.27	-	14.3
	1b	0	22.8	-
	2a	0.31	-	14.0
	2b	0	21.4	-
	3a	0.27	-	13.8
	3b	0	20.6	-

4 ANALYSIS

4.1 *Correlation between $f_{c,0,meas,wet}$ and KR*

The correlation between $f_{c,0,meas,wet}$ and KR measured with Φ_1 is shown in Figure 5. However, the trend line gives a zero strength value for a KR lower than 1, indicating that only taking the size of Φ_1 is not sufficient to describe a zero strength zone caused by a knot. Therefore, in Figure 6, the correlation between $f_{c,0,meas,wet}$ and Φ_2 showed that for Φ_2, calculated according to Equation 1, the factor β is optimized in such a way that for KR (Φ_2) = 1, the value for $f_{c,0,meas,wet}$ = 0. In order to achieve this, a value of β = 0.462 was determined. This means that the equivalent zero strength zone of a knot (taking into account the knot itself and the fiber deviation around it), which is assumed to take up no load, is defined by Φ_1 plus approximately half of Φ_1. The R^2 values found in Figures 5 and 6 are similar, which can be explained from the fact that most knots fell in class C according to Table 1, with a value of $\alpha \approx 1$. Thus, the influence of knots as a strength reducing factor on the load bearing capacity of timber piles, will be studied with KR (Φ_2). The values of KR (Φ_2) in relation to $f_{c,0,KR,meas,wet}$ and $f_{c,0,CW,meas,wet}$ determined for the tested discs, were also added in Figure 6, resulting to be in line with the values obtained from the pile segments. However, this subject is part of further investigation by testing more discs in the future.

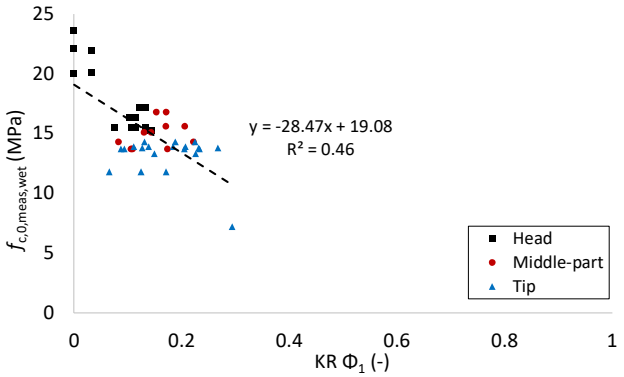

Figure 5. Correlation between $f_{c,0,meas,wet}$ and KR calculated with Φ_1 for pile segments divided in head, middle-part and tip.

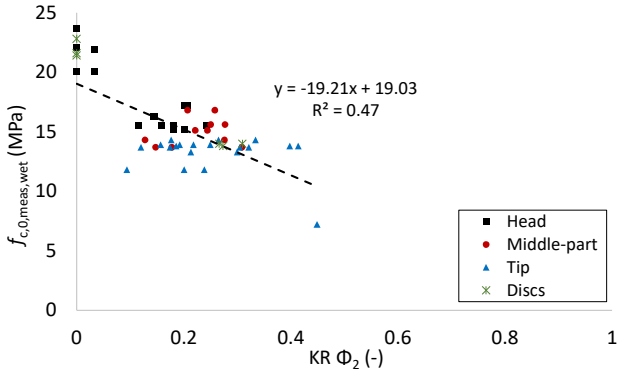

Figure 6. Correlation between $f_{c,0,meas,wet}$ and KR calculated with Φ_2 for pile segments divided in head, middle-part and tip, and discs.

4.2 *Modeling of the compressive strength based on the dry density and KR.*

On the basis of the comparison of the compressive strength obtained from discs with knots (although on a limited amount of tests), it was concluded that the strength of a segment with a certain branch whorl was similar to the strength of the branch whorl disc itself. The discs without knots had similar strength as segments without knots. Thus, the discs sawn from a clear wood section of the pile, showed $f_{c,0,CW,meas,wet}$ values which could be adopted, in combination with KR (Φ_2), to predict the failure at any position of a full-length pile. For the parts without knots it is assumed

that this basic strength is related to the dry density, based on the research of Ravenshorst (2015), where this approach was adopted for bending strength. On this basis, the prediction of $f_{c,0,KR,meas,wet}$ could be done in any section of a pile, once KR and dry density of that pile are known. The influence that knots could have on $f_{c,0,meas,wet}$ was calibrated on the basis of mechanical properties of samples without knots, with reference to dry density (for a m.c. of 0%). To this end, a linear regression analysis was conducted, based on experimental data collected by testing in compression five pile segments without knots. Equation 3 shows the prediction equation used for $f_{c,0,CW,mod,wet}$. The error was calculated considering a level of confidence of 99% given the few samples used.

$$f_{c,0_{CW,mod,wet}} = C_1\ \rho_{dry} + C_{k,1} + \varepsilon_{k,1} \quad (3)$$

where C_1 = experimental factor; ρ_{dry} = dry density; $C_{k,1}$ = experimental factor; $\varepsilon_{k,1}$ = error term in regression.

The results in terms of mechanical properties and their correlation with knots, acquired with 110 pile segments, were used to implement a prediction model including the knot ratio KR (Φ_2). Equation 3 was extended with KR (Φ_2) to account for the influence of knots on compressive strength. It is assumed that with the term ($1 - C_2$ KR) the reduction of the active cross section is taken into account (Eq. 4). In this case, the error was calculated with a level of confidence of 95% since 105 specimens were considered.

$$f_{c,0_{KR,mod,wet}} = (C_1\ \rho_{dry} + C_{k,1})(1 - C_2\ KR) + \varepsilon_{k,2} \quad (4)$$

where C_2 = experimental factor; $\varepsilon_{k,2}$ = error term in regression.

The prediction model described by Equations 3-4, was calibrated on five specimens without knots, resulting in $C_1 = 0.028$, $C_{k,1} = 9.62$, $\varepsilon_{k,1} = 3.6$ MPa (Eq. 3); $C_2 = 1$, $\varepsilon_{k,2} = 3.7$ MPa (Eq. 4). This resulted in Equation 5, representing $f_{c,0,KR,meas,wet}$ (Fig. 7).

$$f_{c,0_{KR,mod,wet}} = (0.027\ \rho_{dry} + 10.1)(1 - 1\ KR) + \varepsilon_{k,2} \quad (5)$$

It should be considered that the values predicted for $f_{c,0,KR,mod,wet}$ were calculated with a dry density (for a m.c. of 0%), since for the wet densities the moisture content was different for every segment, and only wood material adds to the strength. Based on that, the coefficients in Equation 5 allow to compare these predicted values with the mechanical properties of water-saturated wooden segments (with m.c. > 60%). The predicted values were slightly underestimated, since the interaction between KR (Φ_2) and density was not taken into account yet.

The formulated prediction model was applied on a full-length pile divided in eight segments, where $f_{c,0,CW,mod,wet}$ was determined with Equation 3, from the density profile shown in Figure 8. The values of $f_{c,0,KR,mod,wet}$ were calculated based on the respective KR (Φ_2) values (Fig. 9) over the length of the pile.

Finally, $f_{c,0,CW,mod,wet}$ and $f_{c,0,KR,mod,wet}$ were plotted in Figure 10, and compared with the actual compressive strength ($f_{c,0,meas,wet}$) determined with mechanical testing on the eight pile segments. The positions where failure occurred during the test are related with the sections with maximum KR for each segment. This can be observed in 75% of cases where the predicted $f_{c,0,KR,mod,wet}$ coincided with $f_{c,0,meas,wet}$ in the section with maximum KR.

It should be noticed that the role played by knots in compressive failure of a pile segment refers to its specific size: the failure location could be different when testing a longer segment, because the maximum KR and its location can vary.

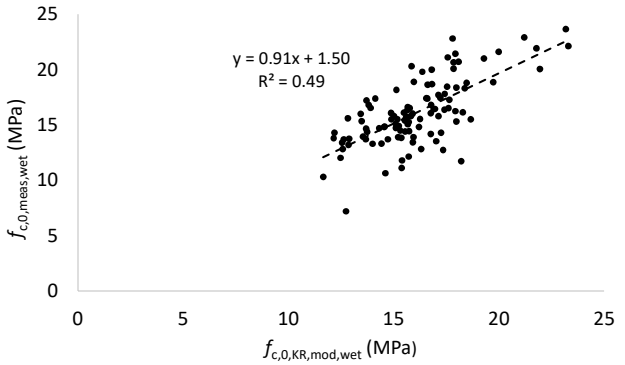

Figure 7. Relationship between $f_{c,0,meas,wet}$ and $f_{c,0,KR,mod,wet}$ calculated with equation 5.

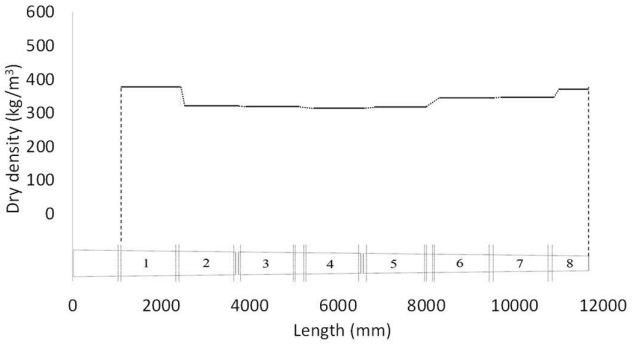

Figure 8. Dry density profile (for a m.c. of 0%) of a full-length pile divided in 8 segments.

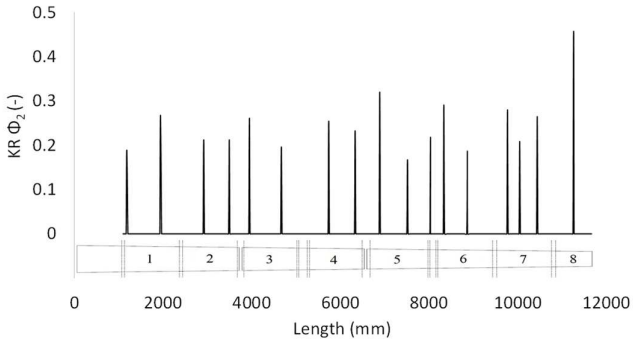

Figure 9. KR (Φ_2) profile of a full-length pile divided in 8 segments.

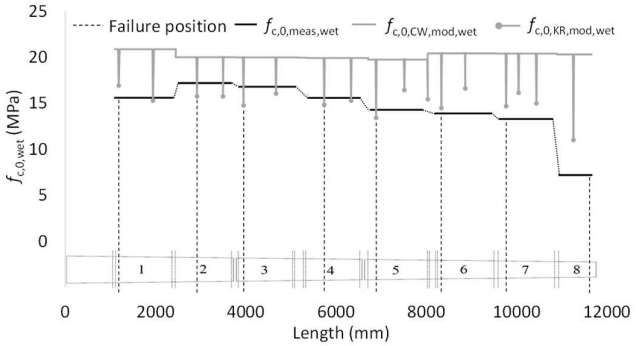

Figure 10. Profile of $f_{c,0,CW,mod,wet}$ calculated from dry density (m.c. = 0%) and $f_{c,0,KR,mod,wet}$ from KR (Φ_2), compared with failure positions of 8 segments along the full pile. The grey lines drawn on the pile represent the cutting positions of the segments.

5 CONCLUSIONS

In this work, the compressive strength ($f_{c,0,meas,wet}$) of wooden foundation piles was studied with full-scale mechanical testing on pile segments in relation with knots layout, expanding on the research of van de Kuilen (1994). The influence of knots on $f_{c,0,meas,wet}$ was determined by comparing the compressive strength of pile segments with and without knots. A correlation was found between $f_{c,0,meas,wet}$ and the area where fibers were deviated by knots, by calculating a knot ratio KR. It was concluded that the equivalent size of the influence of a knot is about 1.5 its diameter, with the assumption that the equivalent area of knots do not contribute to the strength of the pile. It was observed that the failure, in a wooden pile segment tested in compression, occurred in more than 70% of the cases, in the section with the maximum KR. Therefore, a total of six wooden discs were sawn from three pile segments, three from clear wood sections and three from sections with maximum KR, and subjected to small-scale compression tests. A good correlation was observed between the failure $f_{c,0,meas,wet}$ of segments and discs. Thus, it was possible to reliably predict the strength of pile segments from discs with maximum KR, confirming the assumption that the knot area governs the resistance to axial loading. The compressive strength of discs without knots was used as a reference value for the prediction of the failure by using KR. Therefore, the KR can be used not only in relation to pile segments, but also for the full-length pile, allowing to identify the critical sections along the length. On the basis of these experimental results, a prediction model was implemented, calibrated on the strength of pile segments without knots. An equation was determined, to estimate the decrease in compressive strength based on the dry density of a pile and on KR. The predicted values showed good agreement with experimental results. The developed model can have in-situ future implications to predict the failure positions of wooden foundation piles in use, for determining their critical sections. This research can serve as basis for future studies, aiming at determining more specific grading classes for wooden foundation piles, opening up the opportunity of a more optimal use of these structural elements.

6 ACKNOWLEDGEMENTS

The authors gratefully acknowledge Cristiana Gambarin and Gabriele De Mori for their help in experimental tests and data analysis, and the municipality of Amsterdam for having funded this project.

REFERENCES

EN 1309-3 2018. Round and sawn timber - Methods of measurements - Part 3: Features and biological degradations, CEN.

EN 13183-1 2002. Moisture content of a piece of sawn timber - Part 1: Determination by oven dry method, CEN.

EN 14251 2003. Structural round timber - Test methods, CEN.

EN 384 2016. Structural timber - Determination of characteristic values of mechanical properties and density, CEN.

EN 408 2010. Timber structures - Test methods - Pull through resistance of timber fasteners, CEN.

ISO 24294 2021. Timber - Round and sawn timber - Vocabulary, International Organization for Standardization (ISO).

NEN 5461 2011. Requirements for timber (KVH 2010) - Sawn timber and round wood - General part, Nederlands Normalisatie-instituut (NEN).

NEN 5491 2010. Quality requirements for timber - Piles - Coniferous timber, Nederlands Normalisatie-instituut (NEN).

Pagella G. et al. 2022. Assessment of retrieved timber foundation piles from bridges in Amsterdam, ICTB plus 2021 (Submitted).

Ravenshorst G.J.P. 2015. Species independent strength grading of structural timber, Doctoral Thesis.

Satoru Y. & Go M. 2007. Digital Image Correlation, EOLSS.

Van de Kuilen J.W.G. 1994. Bepaling van de karakteristieke druksterkte van houten heipalen. TNO-report 94-CON-R0271, 1994 (in Dutch).

Van de Kuilen J.W.G. et al. 2021. An integral approach for the assessment of timber pile foundations, WCTE 2021.

Vieira Rocha M.F. et al. 2018. Wood knots influence the modulus of elasticity and resistance to compression, Floresta e Ambiente. 25. 10.1590/2179-8087.090617.